Wave dispersion relations in two-dimensional Yukawa systems

Yanhong Liu,[1,*] Bin Liu,[1] Yanping Chen,[1] Si-Ze Yang,[1] Long Wang,[1] and Xiaogang Wang[2]

[1]*Institute of Physics, Chinese Academy of Sciences, Beijing 100080, China*

[2]*State Key Laboratory of Materials Modification by Beams, Department of Physics, Dalian University of Technology,*

Dalian 116024, China

Collective modes in a two-dimensional Yukawa system are investigated by molecular dynamics simulation in a wide range of coupling parameter Γ and screening strength κ. The dispersion relations and sound speeds of the transverse and longitudinal waves obtained for hexagonal lattice are in agreement with the theoretical results. The negative dispersion of the longitudinal wave is demonstrated. Frequency gaps are found on the dispersion curves of the transverse wave due to scattering of the waves on lattice defects for proper values of Γ. The common frequency of transverse and longitudinal waves drops dramatically with the increasing screening strength κ.

I. INTRODUCTION

A collection of charged particles interacting through the screened Coulomb potential $\phi(r) = (Q^2/4\pi\varepsilon_0 r)\exp(-r/\lambda_D)$ is called a Yukawa system, where Q is the particle charge, r is the interparticle distance, and λ_D is the screening length. In general, strongly coupling dusty plasmas [1] and colloidal crystals [2] can be modeled by the Yukawa system. An example of two-dimensional (2D) Yukawa systems is a monolayer of micron size grains trapped in the sheath of gaseous discharges. In such a Yukawa system, the contribution of ions and electrons can be taken into account as the Debye shielding to the charged particle. A Yukawa system is characterized by two dimensionless parameters: the screening strength $\kappa = a/\lambda_D$, i.e., the ratio of the average interparticle distance a to the screening length and the coupling parameter $\Gamma = Q^2/(4\pi\varepsilon_0 a k_B T)$, where T is the system temperature. When $\Gamma \gg 1$ and $\kappa \sim 1$, the particles strongly interact with each other, and form a plasma crystal [3,4]. In the two-dimensional case, it is usually a hexagonal lattice.

The dynamical behavior of Yukawa systems has recently attracted special attention of dusty plasma scientists [5–7]. The collective modes, especially wave dispersions were investigated in experiments and numerical simulations [8–10]. Certain theoretical models also proposed to predict the waves in dusty plasmas [11–13]. Recently, some theoretical and experimental results show that the longitudinal and transverse waves can propagate in the plasma crystal [14–18]. Though there were molecular dynamics (MD) simulations of wave dispersion for dusty plasmas [19–21], the dispersion relation of lattice waves propagating in 2D dusty plasma and the effects of the screening strength on the dispersion relations are, however, not investigated in detail, particularly in a wide range of coupling parameter Γ and screening strength κ. In this paper, we study the collective motions in 2D dusty plasmas by MD simulations, and obtain the dispersion relation for different wave branches and Γ, κ. In most experiments of wave dispersion in the dusty plasma, an external disturbance such as a laser pushing is needed [15,16]. In our simulations, we measured the current correlation functions as in Refs. [19–21] to investigate the collective modes naturally existing in a 2D Yukawa system with finite temperature. Such modes have been reported in a recent experiment [16].

II. METHOD OF MOLECULAR DYNAMICS SIMULATIONS

Our molecular dynamics simulations are performed in a canonical ensemble with 256 particles in a two-dimensional square box of side $L = 16a$ under a periodic boundary condition. The Ewald summation is used in the MD simulation. The cutoff distance of the particle-particle pair interaction potential is chosen as $r_c = L$. The interactions of a given particle i with other particles j and the periodic image of particles j are considered to calculate the electrostatic potential in the MD simulations. The Nosé-Hoover thermostat scheme [22] is used to keep the system at a constant temperature. The time step is $0.1\omega_{pd}^{-1}$, where $\omega_{pd} = \sqrt{Q^2/\varepsilon_0 M a^3}$ is the dusty plasma frequency. The initial runs last about 3×10^4 steps for equilibrium, and in subsequent 2×10^4 time steps, the current correlation functions and their Fourier transformations are computed. The transverse and longitudinal current correlation functions and their Fourier transformations are defined by [19–21]

$$C_t(q,t) = \frac{1}{2N}\langle[\vec{q}\times\vec{j}_q(t)]\cdot[\vec{q}\times\vec{j}_{-q}(0)]\rangle, \tag{1}$$

$$C_l(q,t) = \frac{1}{N}\langle[\vec{q}\cdot\vec{j}_q(t)][\vec{q}\cdot\vec{j}_{-q}(0)]\rangle, \tag{2}$$

$$\tilde{C}_{t,l}(q,\omega) = \int_0^\infty e^{i\omega t}C_{t,l}(q,t)dt, \tag{3}$$

where $q = |\vec{q}| = |\vec{k}a|$ is the normalized wave number. The current $\vec{j}_q(t) = \Sigma_{m=1}^N \vec{v}_m(t)e^{i\vec{q}\cdot\vec{r}_m(t)}$, where $\vec{v}_m(t)$ and $\vec{r}_m(t)$ are the velocity and position of the mth particle at time t,

*Email address: yhliu@aphy.iphy.ac.cn

　　　　　　67 066408-1

respectively. From the peaks and corresponding wave numbers and corresponding wave numbers and corresponding wave numbers and corresponding wave numbers and corresponding wave numbers and corresponding wave numbers in the Fourier transformation spectra, one can obtain the dispersion relations of the different transverse and longitudinal waves.

III. SIMULATION RESULTS AND DISCUSSIONS

A. Wave dispersion relations with different coupling parameters Γ

In a high-Γ Yukawa system, the 2D particle system becomes anisotropic when it begins to "freeze," as shown in Fig. 1(a), and thus not only longitudinal waves but also transverse waves can propagate in it. In a hexagonal crystal, transverse and longitudinal waves can propagate along two independent directions parallel ($\theta=0$) and perpendicular ($\theta=\pi/2$) to the primitive translation vector of the crystal. Therefore, the spectra of the parallel and the perpendicular waves are calculated for transverse and longitudinal modes, respectively. It can also be expected that as Γ varies, the spectra and dispersion relations will go through significant changes.

In Figs. 2(a_1)–2(d_1), the parallel and perpendicular wave spectra of the transverse and longitudinal current correlation functions for $\Gamma=1000$ and $\kappa=1.0$ are shown. The dispersion relations for the four wave branches are obtained from the peaks and corresponding wave numbers in the wave spectra and shown in Figs. 3(a) and 3(b). The theoretical results for a two-dimensional perfect hexagonal crystal and infinite Γ [14,15] are also plotted in Figs. 3(a) and 3(b) for comparison. From Figs. 3(a) and 3(b) one can see that in this strongly coupled regime, the simulation results are in a good agreement with the theoretical predictions, particularly for the long wavelength modes. However, for the short wavelength modes, there are some discrepancies between the simulation and theoretical results which may be caused by the effects of crystal defects [as shown in Fig. 1(a)] and the finite system temperature. It is noted that the defect configuration is random, but the defect size is almost not changed in the simulation. The defect configuration does not depend on the initial conditions either, such as the initial system temperature. Figure 3(a) shows the dispersion relations of two perpendicular modes. The dispersion curves have a maximum at $q=ka=2\pi/\sqrt{3}=3.63$, and are symmetrical to this maximum. This can be explained by the formation of standing waves at the boundary of the first Brillouin zone. Figure 3(b) shows the dispersion relations of two parallel modes. The maximum of the transverse dispersion curve is located at $q=2\pi$. The longitudinal dispersion has a minimum at $q=2\pi$, as well as a maximum at $q=2.35$, and the longitudinal dispersion between the two points is "negative," i.e., the directions of the phase velocity and the group velocity are opposite.

The unique features such as the negative dispersion of the parallel longitudinal modes can be understood in a following simple model. A chain of particles in phase is linked to the nearest-neighbor chain of in-phase particles by a "weak spring," with a very small, in some cases even a "negative" if $\kappa<(1+\sqrt{5})/2$, spring constant. The chain is, on the other hand, linked to the second nearest-neighbor "in-phase chain" with a "strong spring," which should be the main
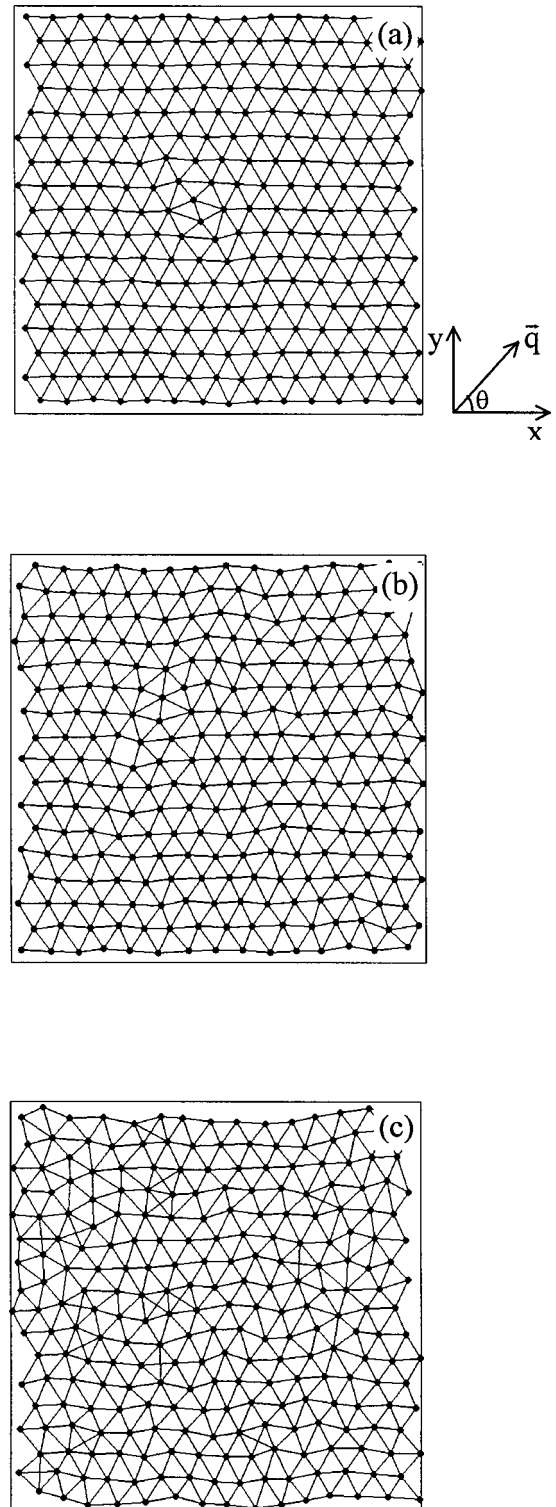

FIG. 1. The lattice structure and nearest-neighbor bonds for (a) $\Gamma=1000$, (b) $\Gamma=144$, and (c) $\Gamma=83$ with $\kappa=1.0$.

energy transfer channel for this mode. In the negative dispersion region, the wavelength is so short that the oscillation phases of neighboring chains of particles are opposite to each other. The direction of the local particle velocity and the group velocity of the wave for alternative chains linked together with the strong spring are opposite to the apparent
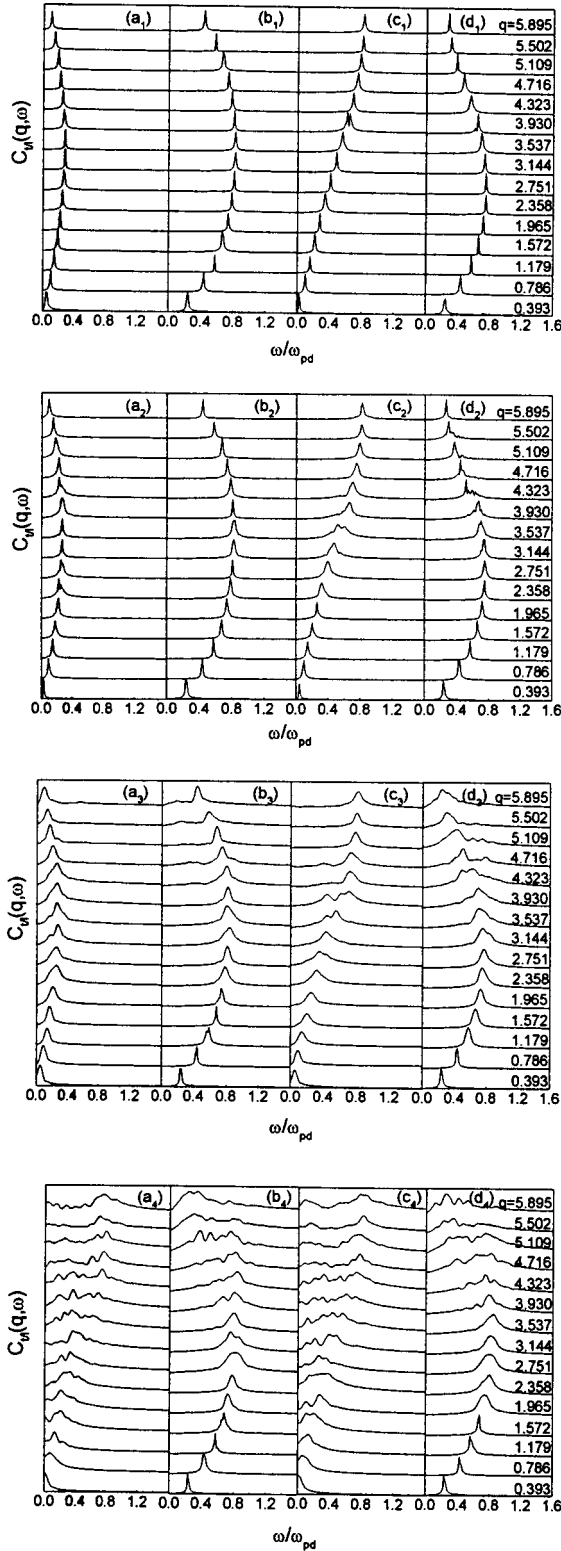
FIG. 2. The parallel ($\theta=0$) and perpendicular ($\theta=\pi/2$) wave spectra of the transverse [$C_t(q,\omega)$] and longitudinal [$C_\ell(q,\omega)$] current correlation functions for different coupling parameters: (a_1) $C_t(q,\omega)$, $\theta=\pi/2$; (b_1) $C_\ell(q,\omega)$, $\theta=\pi/2$; (c_1) $C_t(q,\omega)$, $\theta=0$; (d_1) $C_\ell(q,\omega)$, $\theta=0$, with $\Gamma=1000$ and $\kappa=1.0$. For (a_2)–(d_2), (a_3)–(d_3), and (a_4)–(d_4), the conditions are the same as in (a_1)–(d_1) except with $\Gamma=144$, 83, and 63, respectively. The q denotes the wave numbers $q=0.393$–5.895 for every wave branch.
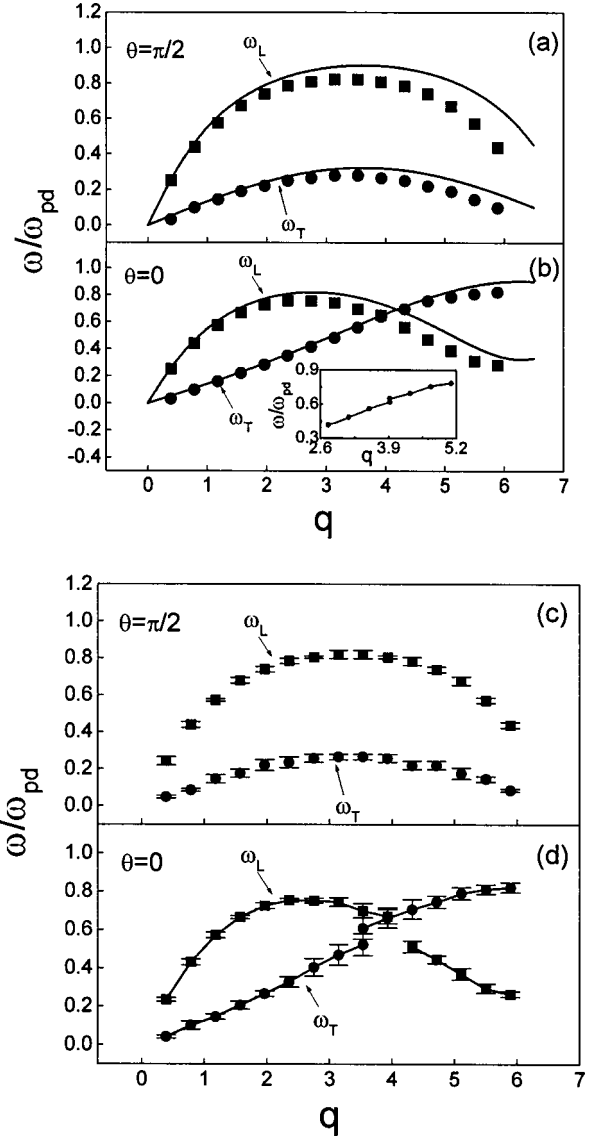

FIG. 3. The dispersion relations of the transverse (ω_T) and longitudinal (ω_L) waves propagating in perpendicular ($\theta=\pi/2$) and parallel ($\theta=0$) directions for different coupling parameters: (a) and (b) for $\Gamma=1000$ and $\kappa=1.0$, where the theoretical curves are obtained from Refs. [10,11]. The inset in (b) shows the detail of the simulation results; (c) and (d) for $\Gamma=144$ and $\kappa=1.0$.

phase velocity. This "alternative spring" model is analogous to optical modes in a two-atom system.

Some fine structures can be observed in the spectra of the parallel waves as shown in Figs. 2(c_1) and 2(d_1). Especially, there is clearly a double peak structure in the spectrum of parallel transverse wave for $q=3.93$, while a similar structure is also observed in that of parallel longitudinal wave, but the second peak is not obvious. The double peak structure for the parallel transverse wave corresponds to a frequency gap in its dispersion relation as shown in an inset in Fig. 3(b). The double peak structure of the parallel transverse wave is possibly caused by the crystal defect effect on the dispersion relation. Let us first test the lattice structure for the case of $\Gamma=1000$ and $\kappa=1.0$ as shown in Fig. 1(a). It was a perfect hexagonal lattice, except for a defect. A wave propagating in

the lattice would be reflected at the defect. Then a standing wave should be formed when the reflected wave superimposed to the incident wave for a certain wave number, which was determined by the size of the lattice defect. Therefore, what was shown in Fig. 3(b) can be referred to as a superposition of the normal mode and a localized mode with only a short wavelength spectrum. In order to verify the hypothesis, we compare the phenomena mentioned above with simulation results for higher Γ, for example, $\Gamma = 10\,000$ and $\kappa = 1.0$. The lattice configuration for this case is a perfect hexagonal lattice without defects, and the fine structures such as double peaks then disappear in the spectra of parallel transverse waves, as shown in Fig. 4. However, the mechanism of wave reflection at the defects will be clarified in detail in the further work. In order to observe the dependence of the numerical results on the computing time and simulating particle number, the simulations are performed again by choosing simulation time steps 1×10^5 and particle number $N = 625$. The initial runs last about 3×10^4 steps for equilibrium, and in subsequent 7×10^4 time steps, the current correlation functions are computed. The simulation results show that the wave spectra are not changed obviously with the increasing computing time and simulating particle number. The width of the spectra peaks does not become wider with increasing wave number. In the one-component plasma, a broad peak structure is observed at finite wave numbers [23], but in a Yukawa system the width of the spectra peaks is not changed significantly with the wave number [21]. The frequency sum rule [24] $\int_{-\infty}^{\infty}(d\omega/2\pi)\omega S(k,\omega) = C\omega(k)$ [$S(k,\omega)$ is the wave spectral function associated with the density correlation function, $\omega(k)$ is the wave frequency corresponding to the wave number k, and C is a constant] is also checked through the relational expression

$$\int_{-\infty}^{\infty}(d\omega/2\pi)\omega S(k_i,\omega)\Big/\int_{-\infty}^{\infty}(d\omega/2\pi)\omega S(k_j,\omega)$$
$$= \omega(k_i)/\omega(k_j)$$

(k_i and k_j are the ith and jth wave numbers, respectively) for some different MD simulation cases, for example, $\Gamma = 1000$, $\kappa = 1.0$, the simulating particle number $N = 256$ and 625, and the computing time is 5×10^4 and 1×10^5 steps (the initial runs last about 3×10^4 steps for equilibrium, and in subsequent time steps, the density correlation functions are computed). The test results show that the frequency sum rule is well fulfilled when the particle number $N = 256$ and the computing time is 1×10^5 steps. When the particle number $N = 256$ and the computing time is taken as 5×10^4 steps, the results have a deviation of about 8% from the case of $N = 256$ and the computing time is 1×10^5 steps. Otherwise, the results do not obviously depend on the simulating particle number. The wave frequencies $\omega(k)$ are not affected by the different computing time and the simulating particle number. Based upon the above discussions, the frequency sum rule is fulfilled in general for the MD simulations.

The relation between lattice defects and frequency gaps is further confirmed with a wide range of Γ. As Γ decreases, the frequency gap reappears. In Figs. 1(b), 2(a$_2$)–2(d$_2$), and
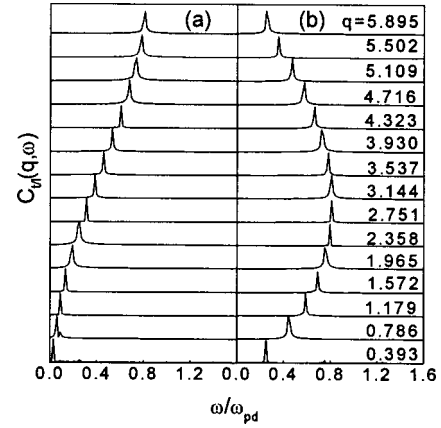

FIG. 4. The parallel ($\theta = 0$) wave spectra of the (a) transverse and (b) longitudinal current correlation functions for $\Gamma = 10\,000$ and $\kappa = 1.0$.

3(c), 3(d), the lattice structure, wave spectra, and dispersion relations are presented for $\Gamma = 144$ and $\kappa = 1.0$. A wider frequency gap appears in the dispersion relation of parallel transverse wave at the wave number $q = 3.537$. Also, similar fine structures can be identified in the perpendicular wave spectra of transverse and longitudinal waves. Obviously, for this parameter group, larger defect structures are found in Fig. 1(b).

In general, the phase transition from the crystalline to the liquid state in a two-dimensional one-component plasma occurs at $\Gamma \approx 137$ [25]. For a Yukawa system, the transition occurs at higher Γ, in particular, for $\kappa = 1.0$, the critical value is about $\Gamma = 272$ for the finite Yukawa system [26]. For the two-dimensional Yukawa system with a periodic boundary condition, the transition critical value may be lower than that of the finite Yukawa system. The system will convert to a liquid as Γ decreases further. Figures 1(c) and 2(a$_3$)–2(d$_3$) present the lattice structure and wave spectra for $\Gamma = 83$ and $\kappa = 1.0$. The wave spectra are similar to that with $\Gamma = 144$, but the peaks of the spectra become much wider. In addition, for the parallel transverse wave the double peak structure seen in Figs. 2(a$_2$)–2(d$_2$) becomes a fluctuationlike structure emerging at the range of $q = 3.537$–3.930 in Figs. 2(a$_3$)–2(d$_3$), and cuts the dispersion curve into two smooth parts. The dispersion of parallel longitudinal wave behaves randomly in the short wavelength region and is getting closer to the perpendicular wave dispersion, which means that the anisotropy becomes weak for this lower Γ. For this case, the number of defects is much high and a large area of irregular structures is formed in the particle configuration, as shown in Fig. 1(c).

As Γ decreases further to 63, most areas of the lattice configuration are covered by irregular structures. The wave spectra shown in Figs. 2(a$_4$)–2(d$_4$) indicate that the anisotropy is no longer obvious. The longitudinal waves in both parallel and perpendicular directions follow the same curve in the long wavelength region and become fluctuating in the short wavelength region. The transverse waves get fluctuated in the whole spectrum. It suggests that transverse waves cannot propagate in the Yukawa system for such a low Γ, the system then is in the liquid phase.
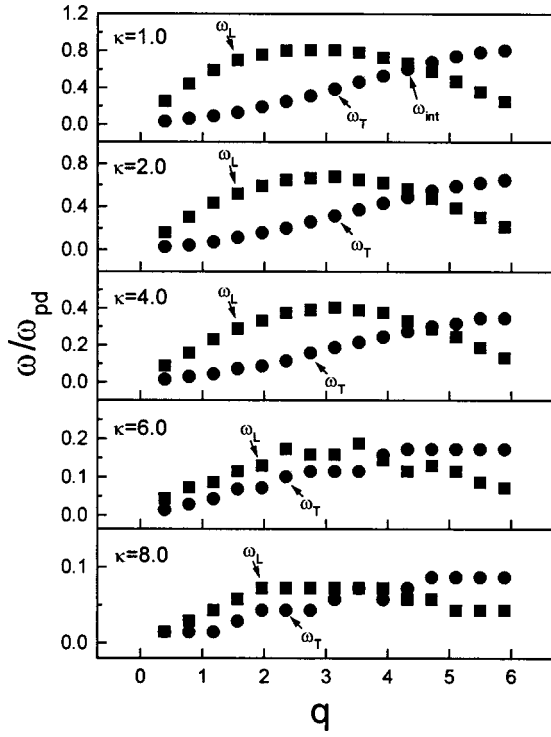
FIG. 5. The dispersion relations of the transverse and longitudinal waves propagating in the parallel ($\theta = 0$) direction for $\Gamma = 10\,000$ and different screening strength κ.

FIG. 6. The longitudinal (C_L) and transverse (C_T) sound speeds as a function of the screening strength κ for $\Gamma = 10\,000$. The sound speeds are in units of $a\omega_{pd}$. The symbols denote the data of the transverse wave (TW) and longitudinal wave (LW) sound speeds obtained from the simulations. The solid curves represent the theoretical results.

From above discussions, one can see that as the coupling parameter Γ varies, the wave spectra and dispersion relations really go through significant changes, and the defects indeed play an important role in the wave dispersion properties.

B. Common frequencies and sound speeds with different screening strength κ

A common feature of dispersion relations of parallel waves shown in Figs. 3(b) and 3(d) separately is that the longitudinal and transverse waves intercross each other at about $q = 4$, providing a common frequency $\omega_{int} \approx 0.64\omega_{pd}$, which is called the Einstein frequency [18]. These figures show that the common frequency is independent of the coupling parameter Γ in the simulation accuracy. In order to investigate the dependence of the common frequency on the screening strength κ, the simulations are performed for $\Gamma = 10\,000$ and $\kappa = 1.0$, 2.0, 4.0, 6.0, and 8.0, respectively. The simulation results are shown in Fig. 5. From Fig. 5, the common frequencies of the parallel transverse and longitudinal waves are obtained as $\omega_{int} = 0.64\omega_{pd}$, $0.52\omega_{pd}$, $0.30\omega_{pd}$, $0.15\omega_{pd}$, and $0.07\omega_{pd}$ for $\kappa = 1.0$, 2.0, 4.0, 6.0, and 8.0, respectively. The simulation results indicate that the common frequency drops dramatically with the increasing screening strength κ. These results can be explained by the following fact that with increasing screening strength κ, the interaction potential $\phi(r) = (Q^2/4\pi\varepsilon_0 ar)\exp(-\kappa r)$ between the dusty particles is reduced greatly, and so the hexagonal lattice gradually becomes disordered, and finally even the transverse wave cannot propagate in the system as discussed
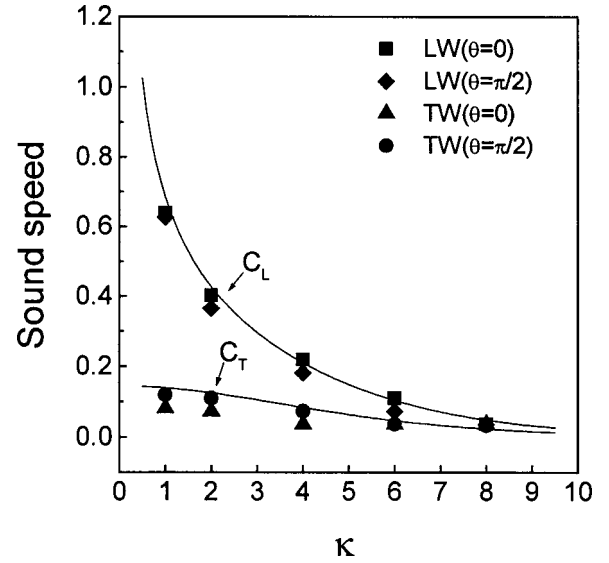
above, so the common frequency also drops dramatically with the increasing screening strength κ.

The other common feature of the wave dispersion relations is that in the limit $q \to 0$, the sound speeds of the transverse and longitudinal waves become isotropic and tend to an acoustic limit [14–17] for certain Γ and κ. Figure 6 shows the sound speeds of the transverse and longitudinal waves as a function of the screening strength κ, with $\Gamma = 10\,000$. The theoretical curves for a perfect hexagonal crystal and infinite Γ are also plotted in Fig. 6 for comparison. From Fig. 6, one can see that the sound speeds are in agreement with the theoretical results [14,27], and the longitudinal and transverse sound speeds gradually decrease with the increasing screening strength κ. These results can also be explained by the changes of lattice structure during the reducing interaction potential (namely, increasing screening strength κ) between the particles as discussed above.

IV. SUMMARY

The transverse and longitudinal wave dispersion relations in a two-dimensional Yukawa system are investigated by molecular dynamics simulation. It is found that the wave dispersion relations and sound speeds obtained in a two-dimensional hexagonal lattice are in agreement with the theoretical results. Negative dispersion is demonstrated for parallel longitudinal lattice waves. It can be understood by a simple "weak-strong" spring coupling model. Frequency gaps are found on the dispersion curves of the transverse wave due to the scattering of the waves on lattice defects for proper values of Γ. The changes in the wave spectra and dispersion relations are monitored by decreasing the coupling parameter. We find that (1) the smooth dispersion curve is "broken" with a frequency gap when lattice defects ap-

pear, (2) as the coupling parameter decreases further, more localized modes caused by wave reflection at defects overlap with each other and form fluctuating structures in the short wavelength region of the dispersion curves, (3) when the system enters the liquid state, the anisotropy disappears. The transverse waves cannot propagate and the longitudinal waves convert to the compressional acoustic wave in a continuous media. The dispersion curves of parallel longitudinal and transverse waves intercross at a common frequency, independent of the coupling parameters. The common frequency drops dramatically with the increasing screening strength κ.

[1] H. Ikezi, Phys. Fluids **29**, 1764 (1986).
[2] C. A. Murray and D. H. Van Winkle, Phys. Rev. Lett. **58**, 1200 (1987).
[3] A. Melzer, T. Trottenberg, and A. Piel, Phys. Lett. A **191**, 301 (1994).
[4] Y. Hayashi and K. Tachibana, Jpn. J. Appl. Phys., Part 2 **33**, L804 (1994).
[5] N. F. Otani, A. Bhattacharjee, and X. Wang, Phys. Plasmas **6**, 409 (1999).
[6] M. S. Murillo, Phys. Plasmas **7**, 33 (2000).
[7] P. K. Kaw, Phys. Plasmas **8**, 1870 (2001).
[8] G. Praburam and J. Goree, Phys. Plasmas **3**, 1212 (1996).
[9] T. Misawa, N. Ohno, K. Asano, M. Sawai, S. Takamura, and P. K. Kaw, Phys. Rev. Lett. **86**, 1219 (2001).
[10] J. H. Chu and I. Lin, J. Phys. D **27**, 296 (1994).
[11] G. Morfill, A. V. Ivlev, and J. R. Jokipii, Phys. Rev. Lett. **83**, 971 (1999).
[12] X. Wang and A. Bhattacharjee, Phys. Plasmas **6**, 4388 (2000).
[13] B. Farokhi, P. K. Shukla, N. L. Tsintsadze, and D. D. Tskhakaya, Phys. Plasmas **7**, 814 (2000).
[14] X. Wang, A. Bhattacharjee, and S. Hu, Phys. Rev. Lett. **86**, 2569 (2001).
[15] X. Wang, Y. Liu, A. Bhattacharjee, and S. Hu, Thin Solid Films **390**, 228 (2001).
[16] S. Nunomura, J. Goree, S. Hu, X. Wang, A. Bhattacharjee, and K. Avinash, Phys. Rev. Lett. **89**, 035001 (2002).
[17] S. Nunomura, J. Goree, S. Hu, X. Wang, and A. Bhattacharjee, Phys. Rev. E **65**, 066402 (2002).
[18] G. Kalman, M. Rosenberg, and H. E. DeWitt, Phys. Rev. Lett. **84**, 6030 (2000).
[19] H. Ohta and S. Hamaguchi, Phys. Rev. Lett. **84**, 6026 (2000).
[20] P. Schmidt, G. Zwicknagel, P. G. Reinhard, and C. Toepffer, Phys. Rev. E **56**, 7310 (1997).
[21] H. Ohta and S. Hamaguchi, Phys. Plasmas **7**, 4506 (2000).
[22] W. G. Hoover, Phys. Rev. A **31**, 1695 (1985).
[23] V. Golubnychiy, M. Bonitz, D. Kremp, and M. Schlanges, Phys. Rev. E **64**, 016409 (2001).
[24] R. D. Puff, Phys. Rev. **137**, A406 (1965).
[25] A. V. Filinov, M. Bonitz, and Yu. E. Lozovik, Phys. Rev. Lett. **86**, 3851 (2001).
[26] H. Totsuji, Phys. Plasmas **8**, 1856 (2001).
[27] A. Melzer, S. Nunomura, D. Samsonov, Z. W. Ma, and J. Goree, Phys. Rev. E **62**, 4162 (2000).